

# An Integrated FTIR-TLC-PCA Approach for an Accurate Classification Model of Kratom Venation

**Azka Muhammad Rusydan<sup>1\*</sup>, Mitsalina Fildzah A<sup>1</sup>, Endang Lukitaningsih<sup>3</sup>, Nanang Fakhrudin<sup>4</sup>**

<sup>1</sup> Bachelor of Pharmacy Program, Faculty of Medicine, Universitas Jenderal Achmad Yani

<sup>2</sup> Department of Pharmaceutical Chemistry, Faculty of Pharmacy, Universitas Gadjah Mada

<sup>3</sup> Department of Pharmaceutical Biology, Faculty of Pharmacy, Universitas Gadjah Mada

Corresponding author: Azka Muhammad Rusydan | Email: azka.m.rusydan@gmail.com

Submitted: 12-11-2024

Revised: 18-07-2025

Accepted: 14-08-2025

## ABSTRACT

Kratom (*M. speciosa*), has a long history of traditional use for various ailments as well as for recreational purposes due to its opioid and psychoactive effects. Nowadays kratom is easily accessible via online markets, with leaf powders commonly categorized by vein color, suggesting different effects despite minimal variations in alkaloid content. To improve the identification and characterization of kratom samples, fingerprinting methods using chemometric tools are increasingly applied in food and pharmaceutical analysis. This study explores a combination of Fourier Transform Infrared Spectroscopy (FTIR) and Thin-Layer Chromatography (TLC) densitometry data, analyzed with Principal Component Analysis (PCA), to develop a model for distinguishing kratom venation and other alkaloid-containing plants. The TLC chromatogram revealed six consistent peaks (R<sub>f</sub> values of 0.17, 0.27, 0.42, 0.73, 0.8, and 0.9), correlating with alkaloids found in kratom. Using PCA, we combined FTIR absorbance values at selected wavenumbers with TLC chromatogram data, resulting in four principal components (PC1, PC2, PC3, and PC4) that explained 84.1%, 9.7%, 2.7%, and 2.5% of the variance, respectively. The resulting score plot demonstrated distinct clustering of samples, which was then verified with cluster analysis. The resulting analysis indicated effective differentiation between kratom vein colors and plant species. The developed FTIR-TLC-PCA model offers a promising approach for sample classification, potentially aiding quality control and authenticity verification in pharmaceutical applications.

**Keywords:** Kratom; chemometric; FTIR spectroscopy; TLC densitometry, authentication

## INTRODUCTION

Kratom (*Mitragyna speciosa*) is an endogenous plant from Southeast Asia that is traditionally used as a treatment for various ailments such as cough, common cold, fever, diarrhea, increased sexual performance, and opium substitute (Singh et al., 2019, 2020). Kratom isolated two alkaloids namely mitragynine and 7-hydroxy mitragynine (7-OH-MG) (Raffa et al., 2013). Mitragynine is well known as a major analgesic alkaloid in Kratom, that exhibit centrally mediated analgesic activity in various pain models (Ya et al., 2019). Kratom's opioid and psychoactive activities lead to its use for recreational purposes (Raffa et al., 2013; Rech et al., 2015). While the dangerous aspects of kratom consumption and its legal status in various countries remained a grey area, kratom has become easily brought via internet vendors (Cinosi et al., 2015; Olsen et al., 2019; Warner et al., 2016). Kratom is traditional medicine in Dayak community, Kalimantan, Indonesia. The National Narcotics Board of Indonesia investigated that Kratom identified as new opioid in Indonesia to risk misappropriation and has negative impacts on health (Muttaqien, 2024). Kratom leaf powder is typically categorized by the color of the leaf veins, with each color marketed to produce different effects, despite minimal differences in alkaloid concentrations (Ramanathan & McCurdy, 2020)

Fingerprint analysis has been gaining popularity in food analysis and authentication using chemometric tools (Karabagias, 2020). Chemometric tools are valuable techniques to interpret of complex chemical data and mathematical methods, such as Principal Component Analysis (PCA) (Miller & Miller, 2005). PCA model could enhance the classification ability to distinguish between different sample groups based on their chemical characteristics (Worley & Powers, 2016). Fourier Transform Infrared Spectroscopy (FTIR) and Thin-Layer Chromatography (TLC) densitometry are two powerful techniques that provide complementary data on the chemical composition and

characteristics of samples (Arifah et al., 2022; Kartini & Azminah, 2012). FTIR captures the molecular fingerprint through vibrational spectra, identifying functional groups and assessing molecular structure. In contrast, TLC densitometry offers separation and quantification of chemical constituents, particularly useful in complex mixtures. Thus, the combination of the two data with the PCA model could increase its effectiveness in analyzing the properties of the dataset (Nascimento et al., 2020). Despite its potential, studies specifically integrating TLC-FTIR with PCA to identify differences between plant samples for pharmaceutical applications remain limited. This study aims to develop a PCA model based on the combination of TLC and FTIR data to profile and distinguish different kratom venations. This research contributes novel insights by enhancing the precision and reliability of TLC-FTIR-PCA for distinguishing plant sample materials offering a simple screening tool for identifying plant samples in pharmaceutical research.

## METHOD

### Materials

Three brands of three different venations of kratom leaf powder (green, red, and white) were purchased from sellers based in Pontianak, West Kalimantan, Indonesia. Methanol, n-hexane, ethyl acetate, acetone and ammonia were purchased from Merck.

### Sample preparation

All samples were ground into fine powder using FOMAC FGD Z1000 grinder and passed through a mesh 60 sieve. Approximately 1 g of kratom powder was accurately weighted, and extracted using GT Sonic R6 Ultrasonic Cleaner with methanol as solvent in accordance to the optimum condition in the previous research (Rusydan et al., 2021).

### TLC-densitometry analysis

The TLC analysis method used is based on research by (Singh et al., 2019). The extract obtained is applied with CAMAG® Linomat 5 and developed in TLC system with hexane: ethyl acetate: ammonia (30:15:1 v/v/v) as the mobile phase and TLC Silica Gel Plates 60 F<sub>254</sub> (merck) as the stationary phase. The chromatograms were then dried and examined with CAMAG ® TLC Scanner 3.

### FTIR Analysis

FTIR absorbance was measured using Thermo Nicolet iS10 FTIR spectrometer with Thermo Smart iTR diamond ATR. The scanning process was performed from 650 cm<sup>-1</sup> to 4000 cm<sup>-1</sup>. The sample window was cleaned with acetone before and after each use. The resolution was 8 with the number of scans was 32. Every sample measurement was performed by the background collection. (Arifah et al., 2022).

### Data Analysis

The TLC chromatogram along with FTIR spectra were subjected to PCA using Minitab® 22 software version 22.1. PCA aims to group correlated variables and replace them with a new group called the principal components which then allowed to see the difference between samples. Cluster Analysis of observation will be conducted to assess samples similarity across variables to verify PCA classification results (Alin, 2010).

## RESULTS AND DISCUSSIONS

### TLC-densitometry analysis

Kratom extracts were tested with TLC-densitometry to gain a chromatogram profile. The R<sub>f</sub> patterns correlate with alkaloids and other compounds found in the kratom, such as mitragynine and 7-hidroxymitragynine (7-HMG) (Ya et al., 2019). The resulting chromatogram showed peaks at R<sub>f</sub>=0,17; 0,27; 0,42; 0,73; 0,8; and 0,9. These peaks are selected due to its consistently showing up in all readings in Figure 1.

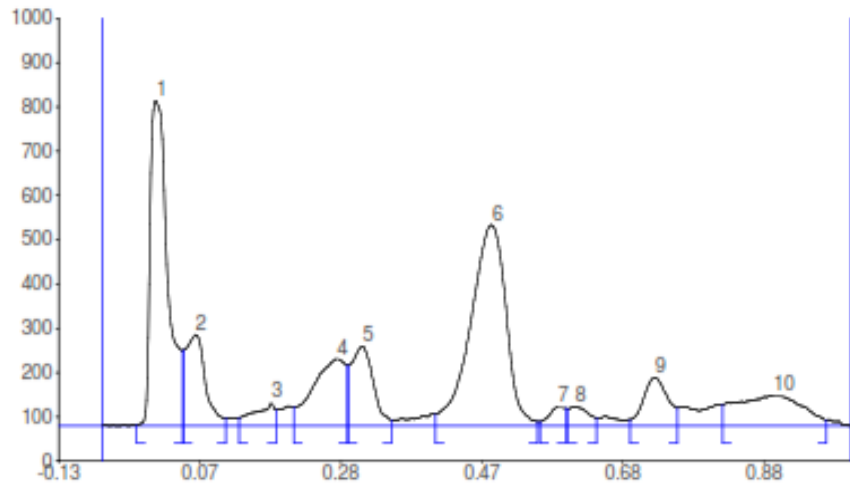


Figure 1. Kratom TLC chromatogram profile

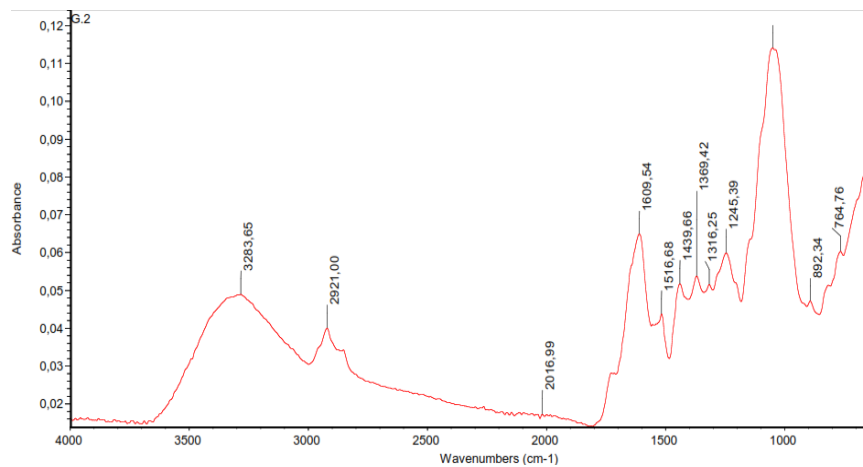


Figure 2. The FTIR spectra of kratom leaf powder

### FTIR Spectral

The FTIR spectra were used to identify the presence of selected functional groups on the mitragynine in Figure 2. The selected wavenumbers investigated the wavenumber of 3285, 65, and 2921,  $1\text{ cm}^{-1}$  categorized -OH and -CH functional group based on C9-hydroxymitragynine structure (Miller & Miller, 2005; Mustafa et al., 2022). (Mustafa et al., 2022) reported that the C22- and C9-hydroxy mitragynine structure at a wavenumber of  $3186\text{ cm}^{-1}$  influenced FTIR spectra related to the hydroxyl compounds group. The ester group of mitragynin was  $1609.54\text{ cm}^{-1}$  attributed to the C=O stretch of carbonyl functional group. The selected wavenumber of  $1245\text{ cm}^{-1}$  and  $1094\text{ cm}^{-1}$  visualized -CO group peak to alcohol/ether group in mitragynin (Mustafa et al., 2022).

### Chemometrics

The variable used in the analysis is the absorbance value of the selected wavenumbers of the FTIR spectra. These wavenumbers are selected based on peaks that are shown in the spectra, thus able to represent unique peaks of kratom. This FTIR spectra data was then combined with a TLC chromatogram and then analyzed using PCA. FTIR provides the molecular fingerprint data, while TLC chromatography adds separation and quantitative data that are not available in FTIR. The combination of FTIR and TLC data provides complementary information, which could improve model accuracy and sensitivity (Kartini et al., 2025).

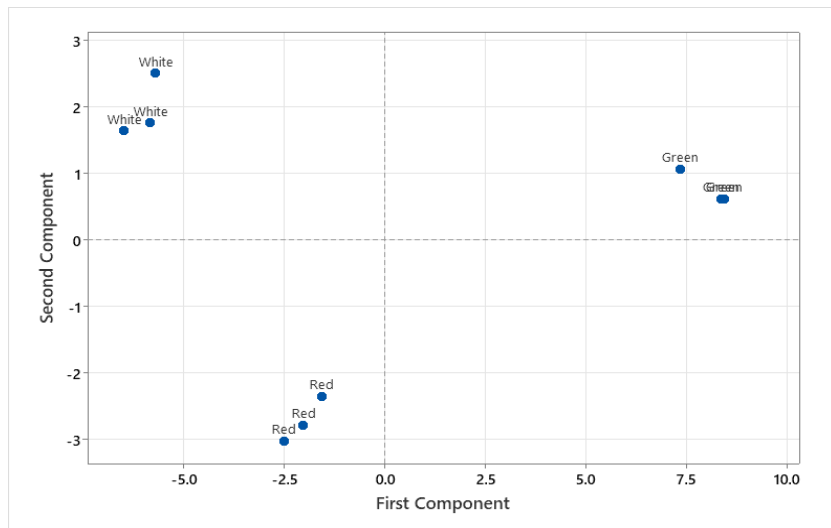


**Figure 3. The PCA Score plot of TLC chromatogram and FTIR spectra data fusion of kratom venation**

**Table I. Eigen analysis table of the correlation matrix. PCs are chosen based on eigenvalue. The higher the eigenvalue, the more PC could capture the dataset.**

	PC1	PC2	PC3	PC4	PC5	PC6	PC7	PC8
<b>Eigenvalue</b>	39.55	4.552	1.252	1.189	0.342	0.08	0.025	0.011
<b>Proportion</b>	0.841	0.097	0.027	0.025	0.007	0.002	0.001	0
<b>Cumulative</b>	0.841	0.938	0.965	0.99	0.998	0.999	1	1

PCA creates a new principal component (PC) variable for classification. To assess the impact of the new PCs, the corresponding eigenvalue is examined. The eigenvalue represents the magnitude of variance captured by PC, and a higher eigenvalue indicates higher significance in capturing the data structure. The PC needs to have eigenvalue  $> 1$  to be selected. Only PC1, PC2, PC3, and PC4 meet the required eigenvalue, which represents 84.1 %, 9.7%, 2.7%, and 2.5% of the total variance respectively. The eigenvector shows the magnitude and direction of the 41 wavenumbers impact on the PCs. PC1 was most impacted by peaks at  $660 - 1550 \text{ cm}^{-1}$  while PC2 was most impacted by peaks at  $1900-3300 \text{ cm}^{-1}$  and TLC AUC value. Meanwhile, PC 3 and PC4 are mainly impacted by the TLC data.

The resulting score plot shows that all samples have different ranges against the first two principal components (PC1 and PC2) in Figure 3. These two are chosen because it is statistically a better representation of total variation in the data set (93.8%) compared to other combinations. The spread of observation can be used to categorize the data based on similarities. The results have shown that the FTIR data used could separate and differentiate the samples into different clusters and even different quadrants. This indicates that the method developed could distinguish kratom venation based on its unique properties. The difference in quadrant may indicate that the PCA used can be used effectively to classify and predict a sample identity based on its unique properties. Differences between samples within the same sample group might be due to variations in the time of harvest and meteorological conditions for each sample (Sengnon et al., 2023).

Cluster analysis on observation results was conducted with PC1 and PC2 as variables to verify the partition for each cluster in Figure 4. Similarity level value  $> 0.7$  commonly used as indicator that there is a significant similarity between cluster section, while distance level  $> 1.5$  might indicate significant dissimilarity between cluster section. Cluster analysis results showed that it contains a total of 9 observations, with six step linkage is within the desired similarity level (92,1297) and distance level (1,1766) with 3 clusters. This indicate that the numbers of clusters sufficient for the

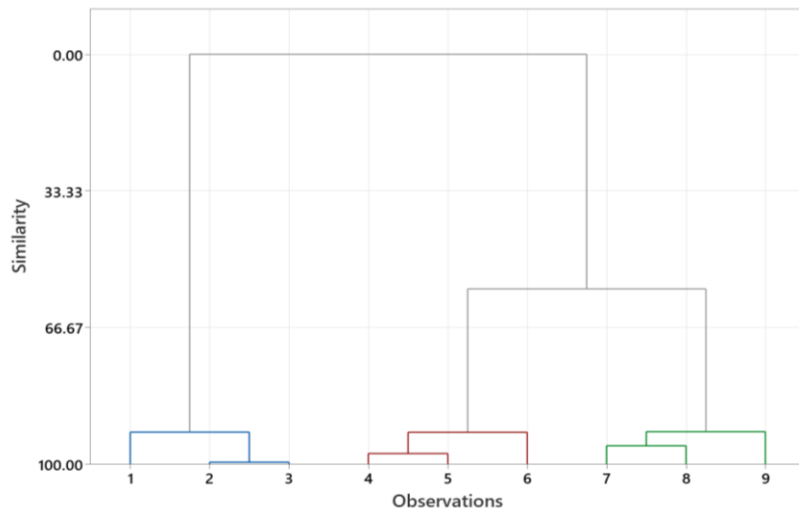


**Figure 4.** The Dendrogram results were categorized in three final partition clusters.

**Table II.** Amalgamation steps of cluster analysis on PCs. The sudden changes of similarity level and distance level indicate that the final partition has been reached.

Step	# of clusters	Similarity level	Distance level	Clusters joined	New cluster	# of obs. in new cluster
1	8	99.5765	0.0633	2	3	2
2	7	97.4505	0.3811	4	5	2
3	6	95.5589	0.6639	7	8	2
4	5	92.2632	1.1566	4	6	3
5	4	92.2219	1.1628	1	2	3
6	3	92.1297	1.1766	7	9	3
7	2	57.2766	6.3869	4	7	6
8	1	0.0000	14.9495	1	4	9

**Table III.** Distance between cluster centroids. Smaller cluster centroids value indicating similarity between two clusters.

	Cluster1	Cluster2	Cluster3
Cluster1	0.0000	10.7293	14.1039
Cluster2	10.7293	0.0000	6.1035
Cluster3	14.1039	6.1035	0.0000

final partition are 3 clusters. The final partition is able to classify each sample correctly, which indicate logical separation were achieved based on the dataset for classification of kratom venation.

The analysis of the cluster centroids further supports the Identified grouping, as each cluster exhibits distinct characteristics associated with specific kratom venation. The clustering aligns with existing literature that suggests different kratom vein colors may correlate with varying concentrations of active compounds, such as mitragynine and 7-hydroxymitragynine (7-HMG) (Hassan et al., 2013; Takayama, 2004). The distance between centroids, were used to evaluate how closely related the clusters are. From the cluster centroids, it was showed that cluster 2 (red) and cluster 3 (white) are closely related. This could be due to similar alkaloids composition between the two venations in comparison to green venation.

While the result of PCA is satisfactory, the dataset in this study was far too little to be divided into a training set and a testing set for prediction. Further sample collection, especially with more diverse sample pools such as differences in the sample region and also different sample identities

could be beneficial for developing a better prediction tool. Adding more relevant variables into the model could improve data representation, thus better capturing the variability in the dataset.

## CONCLUSIONS

This study investigated the use of TLC chromatograms and FTIR spectra of kratom combined with chemometrics could differentiate and classify based on different kratom venations. The combined dataset provided a complementary method to classify kratom venation. However, further research focusing on a more diverse dataset needs to be done to develop a better prediction model. However, this study also showed the potential of TLC-densitometry and FTIR spectroscopy coupled with chemometrics as tools for the classification of kratom venation.

## ACKNOWLEDGEMENT

The completion of this research would not have been possible without the financial support of Faculty of Pharmacy Universitas Gadjah Mada through its research grant program.

## REFERENCES

Alin, A. (2010). Minitab. *Wiley Interdisciplinary Reviews: Computational Statistics*, 2(6), 723–727. <https://doi.org/10.1002/wics.113>

Arifah, M. F., Hastuti, A. A. M. B., & Rohman, A. (2022). Utilization of UV-visible and FTIR spectroscopy coupled with chemometrics for differentiation of Indonesian tea: an exploratory study. *Indonesian Journal of Pharmacy*, 33(2). <https://doi.org/10.22146/ijp.3795>

Cinosis, E., Martinotti, G., Simonato, P., Singh, D., Demetrovics, Z., Roman-Urrestarazu, A., Bersani, F. S., Vicknasingam, B., Piazzon, G., Li, J.-H., Yu, W.-J., Kapitány-Fövény, M., Farkas, J., Di Giannantonio, M., & Corazza, O. (2015). Following “the Roots” of Kratom (*Mitragyna speciosa*): The Evolution of an Enhancer from a Traditional Use to Increase Work and Productivity in Southeast Asia to a Recreational Psychoactive Drug in Western Countries. *BioMed Research International*, 2015, 1–11. <https://doi.org/10.1155/2015/968786>

Hassan, Z., Muzaimi, M., Navaratnam, V., Yusoff, N. H. M., Suhaimi, F. W., Vadivelu, R., Vicknasingam, B. K., Amato, D., von Hörsten, S., Ismail, N. I. W., Jayabalan, N., Hazim, A. I., Mansor, S. M., & Müller, C. P. (2013). From Kratom to mitragynine and its derivatives: Physiological and behavioural effects related to use, abuse, and addiction. *Neuroscience & Biobehavioral Reviews*, 37(2), 138–151. <https://doi.org/10.1016/j.neubiorev.2012.11.012>

Karabagias, I. K. (2020). Advances of spectrometric techniques in food analysis and food authentication implemented with chemometrics. *Foods*, 9(11). <https://doi.org/10.3390/foods9111550>

Kartini, & Azminah. (2012). Chromatographic fingerprinting and clustering of *Plantago major* L. from different areas in Indonesia. *Asian Journal of Pharmaceutical and Clinical Research*, 5, 191–195.

Kartini, K., Ariyani, V. M., Ang, W., Aini, Q., Jayani, N. I. E., Oktaviyanti, N. D., Setiawan, F., & Azminah, A. (2025). A Validated TLC-Densitometric Analysis of Curcumin in Eight Important Zingiberaceae Rhizomes and Their ATR-FTIR Fingerprint Profiles. *Food Analytical Methods*, 18(5), 717–731. <https://doi.org/10.1007/s12161-024-02747-x>

Miller, J. C., & Miller, J. N. (2005). *Chemometrics for Analytical* (5th ed.). Pearson Education Limited.

Mustafa, R. R., Sukor, R., Mohd Nor, S. M., & Saari, N. (2022). Methyl ester and aromatic ether modification of mitragynine for generation of mitragynine-specific polyclonal antibodies. *Journal of Immunological Methods*, 507, 113291. <https://doi.org/10.1016/j.jim.2022.113291>

Muttaqien, M. Z. (2024). Pandangan BNN terhadap Penggunaan Tanaman Kratom pada komunitas Dayak di Kalimantan Barat. *Syntax Idea*, 6(9), 4064–4069. <https://doi.org/10.46799/syntax-idea.v6i9.4488>

Nascimento, L. E. S., Arriola, N. D. A., da Silva, L. A. L., Faqueti, L. G., Sandjo, L. P., de Araújo, C. E. S., Biavatti, M. W., Barcelos-Oliveira, J. L., & de Mello Castanho Amboni, R. D. (2020). Phytochemical profile of different anatomical parts of jambu (*Acmeella oleracea* (L.) R.K.

Jansen): A comparison between hydroponic and conventional cultivation using PCA and cluster analysis. *Food Chemistry*, 332. <https://doi.org/10.1016/j.foodchem.2020.127393>

Olsen, E. O., O'Donnell, J., Mattson, C. L., Schier, J. G., & Wilson, N. (2019). Notes from the Field: Unintentional Drug Overdose Deaths with Kratom Detected — 27 States, July 2016–December 2017. *MMWR. Morbidity and Mortality Weekly Report*, 68(14), 326–327. <https://doi.org/10.15585/mmwr.mm6814a2>

Raffa, R. B., Beckett, J. R., Brahmbhatt, V. N., Ebinger, T. M., Fabian, C. A., Nixon, J. R., Orlando, S. T., Rana, C. A., Tejani, A. H., & Tomazic, R. J. (2013). Orally Active Opioid Compounds from a Non-Poppy Source. *Journal of Medicinal Chemistry*, 56(12), 4840–4848. <https://doi.org/10.1021/jm400143z>

Ramanathan, S., & McCurdy, C. R. (2020). Kratom (*Mitragyna speciosa*): worldwide issues. *Current Opinion in Psychiatry*, 33(4), 312–318. <https://doi.org/10.1097/YCO.0000000000000621>

Rech, M. A., Donahey, E., Cappiello Dziedzic, J. M., Oh, L., & Greenhalgh, E. (2015). New Drugs of Abuse. *Pharmacotherapy: The Journal of Human Pharmacology and Drug Therapy*, 35(2), 189–197. <https://doi.org/10.1002/phar.1522>

Rusydan, A. M., Lukitaningsih, E., & Fakhrudin, N. (2021). Modeling and Optimization of *Mitragyna speciosa* Extraction using Box Behnken Design. *Majalah Obat Tradisional*, 26(3), 204. <https://doi.org/10.22146/mot.68610>

Sengnon, N., Vonghirundecha, P., Chaichan, W., Juengwatanatrakul, T., Onthong, J., Kitprasong, P., Sriwiriyajan, S., Chitrakarn, S., Limsuwanchote, S., & Wungsintawekul, J. (2023). Seasonal and Geographic Variation in Alkaloid Content of Kratom (*Mitragyna speciosa* (Korth.) Havil.) from Thailand. *Plants*, 12(4), 949. <https://doi.org/10.3390/plants12040949>

Singh, D., Grundmann, O., Murugaiyah, V., Rahim, A. B. M., Chawarski, M., & Balasingam, V. (2020). Improved sexual functioning of long-term daily users of *Mitragyna speciosa* (Korth.). *Journal of Herbal Medicine*, 19, 100293. <https://doi.org/10.1016/j.hermed.2019.100293>

Singh, D., Narayanan, S., Müller, C. P., Swogger, M. T., Chear, N. J. Y., Dzulkapli, E. Bin, Yusoff, N. S. M., Ramachandram, D. S., León, F., McCurdy, C. R., & Vicknasingam, B. (2019). Motives for using Kratom (*Mitragyna speciosa* Korth.) among regular users in Malaysia. *Journal of Ethnopharmacology*, 233, 34–40. <https://doi.org/10.1016/j.jep.2018.12.038>

Takayama, H. (2004). Chemistry and Pharmacology of Analgesic Indole Alkaloids from the Rubiaceous Plant, *Mitragyna speciosa*. *Chemical and Pharmaceutical Bulletin*, 52(8), 916–928. <https://doi.org/10.1248/cpb.52.916>

Warner, M. L., Kaufman, N. C., & Grundmann, O. (2016). The pharmacology and toxicology of kratom: from traditional herb to drug of abuse. *International Journal of Legal Medicine*, 130(1), 127–138. <https://doi.org/10.1007/s00414-015-1279-y>

Worley, B., & Powers, R. (2016). PCA as a Practical Indicator of OPLS-DA Model Reliability. *Current Metabolomics*, 4(2), 97–103. <https://doi.org/10.2174/2213235x04666160613122429>

Ya, K., Tangamornsuksan, W., Scholfield, C. N., Methaneethorn, J., & Lohitnavy, M. (2019). Pharmacokinetics of mitragynine, a major analgesic alkaloid in kratom (*Mitragyna speciosa*): A systematic review. *Asian Journal of Psychiatry*, 43, 73–82. <https://doi.org/10.1016/j.ajp.2019.05.016>